Received April 2002
Revised August 2002
Accepted January 2003

# Multi-domain DRM boundary element method for non-isothermal non-Newtonian Stokes flow with viscous dissipation

W. Florez
*Energy and thermodynamics Institute, Bolivariana University, Colombia*
H. Power
*School of Mechanical, Material, Manufacturing Engineering and Managment. The University of Nottingham, University Park, UK*
F. Chejne
*Energy and thermodynamics Institute, Bolivariana University, Colombia*

***Keywords*** *Boundary element methods, Fluid dynamics, Heat transfer*

***Abstract*** *This paper presents a boundary element method (BEM) based on a subdomain approach for the solution of non-Newtonian fluid flow problems which include thermal effects and viscous dissipation. The volume integral arising from non-linear terms is converted into equivalent boundary integrals by the multi-domain dual reciprocity method (MD-DRM) in each subdomain. Augmented thin plate splines interpolation functions are used for the approximation of field variables. The iterative numerical formulation is achieved by viewing the material as divided into small elements and on each of them the integral representation formulae for the velocity and temperature are applied and discretised using linear boundary elements. The final system of non-linear algebraic equations is solved by a modified Newton's method. The numerical examples include non-Newtonian problems with viscous dissipation, temperature-dependent viscosity and natural convection due to bouyancy forces.*

## 1. Introduction

The main purpose of this work is to present the use of the multi-domain dual reciprocity method (MD-DRM) (Florez and Power, 2001a; Popov and Power, 1999) for the numerical simulation of inelastic non-Newtonian flow with viscous dissipation effects and with a viscosity dependent on both the rate of deformation and temperature. The MD-DRM is a recently developed technique that allows an efficient and accurate boundary element numerical solution of highly non-linear and convective problems.

The authors would like to thank COLCIENCIAS (Colombian Science Foundation) for their financial support under the grant 470-2000.

International Journal of Numerical Methods for Heat & Fluid Flow
Vol. 13 No. 6, 2003
pp. 736-768

0961-5539
DOI 10.1108/09615530310498402

For liquids with high viscosity and low thermal conductivity such as most polymers, viscous dissipation cannot be neglected because it has a strong influence on the temperature field which in turn affects the thermophysical properties of the fluid. This phenomenon is particularly relevant to the polymers processing industry (in extrusion and injection processes the fluid is forced to flow through channels where high power generation near the walls is observed (Davis, 1995). Also in radiator design, where the working fluids are usually highly viscous oils, dissipation in laminar flow regime is important.

The behavior of non-Newtonian fluids is strongly dependent on the viscosity variations within the domain which are caused by the shear rate and temperature. Most non-Newtonian fluids like polymers exhibit a viscosity that is a decreasing function of the shear rate, this characteristic is known as shear thinning (Agassant *et al.*, 1991). The viscosity of an inelastic non-Newtonian fluid can be calculated on the one hand in terms of the shear rate through several mathematical models such as the power law model; the Carreau model and the hyperbolic tangent model (Agassant *et al.*, 1991; Bird *et al.*, 1960). On the other hand, the viscosity of polymer melts changes drastically with temperature (a change of 1 percent in temperature can cause at least a 25 percent change in viscosity) and it can be calculated by either the Andrade law (Agassant *et al.*, 1991), or the WLF equation (Agassant *et al.*, 1991). Since the viscosity of non-Newtonian fluids is dependent on shear rate and temperature, it follows that the mathematical models governing the flow motion are non-linear even in the case when inertia effects can be neglected, i.e. at low Reynolds number. This type of flow process requires sophisticated numerical solution techniques.

There is another subset of fluid flow problems called natural convection, where the flow pattern is due to buoyancy forces caused by temperature differences. To our knowledge, the fully developed laminar convection problem including both viscous dissipation and buoyancy effects has not already been solved by using the boundary element method (BEM). In this work, we will present how the MD-DRM technique can be used to solve this type of problems, showing the efficiency and versatility of the proposed numerical approach. The obtained numerical solution to the above mentioned case will be compared with the solution obtained by a perturbation method presented by Barletta (1998) for one-dimensional flow between parallel plates.

The application of the BEM to non-Newtonian and non-linear problems requires finding a fundamental solution of the system of governing equations. However, since such fundamental solution for a general model is not possible to be known, it is necessary to put the non-linear terms into a pseudo-body force leading to domain integrals that can be evaluated by using the cell integration approach (Cell-BEM) (Brebbia *et al.*, 1984). Although this method is effective and general, it makes the BEM lose its boundary only nature resulting in a numerical scheme of several orders of magnitude and more time consuming

than other domain techniques such as the finite differences (FDM) and finite element methods (FEM). The computational cost of the cell integration approach mainly depends on the fact that the solution at each surface or internal point must involve the evaluation of the complete surface integrals yielding in this way to a fully populated matrix system.

A handful of methods have been developed to take the domain integrals to the boundary. Among them, the dual reciprocity method (DRM) (Partridge *et al.*, 1992) and the particular solution method (PIT) (Nardini and Brebbia, 1982) are the most popular ones. These two approaches have been particularly attractive in recent years because of the advances in multidimensional interpolation with radial basis functions (RBF) used in these techniques. Both the DRM and PIT approximate the non-linear and non-homogeneous terms of a partial differential equation as a series of vector valued interpolation functions, which are defined in terms of a set of surface and internal nodes. These interpolation functions lead to a particular solution for the problem which can be used together with Green's identities to convert the domain integrals into boundary integrals. As in the cell integration approach, in these two boundary approaches only the evaluation of the functions at each node requires the integration of the complete surface integrals yielding again a fully populated matrix system.

A major problem encountered with the DRM and PIT is that the resulting algebraic system consists of a series of matrix multiplications of dense matrices. Although the computing time required by the DRM and PIT, when few or no internal points are used, is lower than with the cell integration scheme, it is still very high compared to domain approaches. Besides, when internal points are required their corresponding computational cost becomes similar or higher than those required by the cell integration approach. On the other hand, in complex problems both the DRM and PIT have been limited to a small degree of non-linearity. From these limitations, it appears that this type of boundary formulations only in their original single domain form cannot be extended to solve highly non-linear problems.

When dealing with the BEM solution of large problems it is usual to use the method of domain decomposition, in which the original domain is divided into sub-regions, and in each of them the full integral representation formula is applied. At the interfaces between the adjacent sub-regions, the corresponding continuity conditions are enforced. While the matrices which arise in the single domain DRM are fully populated, the sub-region formulation leads to block banded matrix systems with one block for each sub-region and overlaps between blocks when sub-regions have a common interface.

The implementation of the subregion BEM formulation in the limiting case of a very large number of subregions, including cell integration at each subregion was called by Taigbenu and collaborators as the Green element method (GEM) (Taigbenu, 1995). In this method, the resultant coefficient

matrix is as sparse as that of the FEM and hence its solution is as efficient as in that domain approach.

Recently, Popov and Power (1999) found that the DRM approximation of the internal potential of a non-linear convection diffusion problem can be substantially improved by using a domain decomposition scheme. Popov and Power's idea of using domain decomposition to improve the accuracy of the DRM approach was inspired by the work of Kansa and Carlson (1995) on data approximation with RBFs. Kansa and Carlson observed that the best approximation is obtained when the original domain is split into matching subdomains. In similar way, Popov and Power (1999) noticed that the DRM approximation for the non-linear problems can also be improved when the original domain is divided into smaller subdomains. At each subregion the BEM formulation of the problem is separately applied. The corresponding domain integral resulting from the BEM formulation is transformed to surface integrals along the contour of the subregions by the DRM approach. The desired accuracy of the scheme is achieved by refining the size of the subdomains. For large number of subdomains this technique was called MD-DRM, and the discrete form of the integral equation formulation of the problem is given by a banded matrix system. Recently the MD-DRM has been successfully applied by Florez and Power (2001b) to the solution of isothermal non-Newtonian flow problems and to the Navier Stokes equations for incompressible Newtonian fluids at moderately high Reynolds numbers (Florez *et al.*, 2000). In the present work, it will be shown how the MD-DRM can be extended to more general non-isothermal non-Newtonian problems including viscous dissipation terms.

The problem of multiplication of several large fully populated matrices encountered in the DRM formulation in a single domain is reduced, in the present domain decomposition case, to the multiplication of very small matrices at each subdomain. Besides, if the subdomains are of similar shape all the evaluations and multiplications can be performed only in one subdomain, and the results for the others can be found by scaling due to the geometric characteristic of the DRM functions. Because of the nature of the integral equation formulation at each subdomain, the solution obtained with MD-DRM is a kind of Hermitian solution. In the present case of non-isothermal and non-Newtonian flow, the values of the velocity and shear stress fields as well as the temperature and its directional derivatives at every point defining the subdomains are found directly from the solution of the resulting matrix system.

Although the solution of a fully populated system of equations is computationally very expensive, this type of solution for a sparse system can be carried out very efficiently by not considering the multiplications of the zero terms. In this manner, the solution of the MD-DRM system could be obtained in a fraction of the solution of an equivalent fully populated system resulting from any of the other standard BEM schemes. Besides, the required storage of the

MD-DRM approach is substantially smaller than the one required by other BEM schemes. For the sparse system obtained with the MD-DRM approach, both the efficiency and the storage requirement, are functions of the bandwidth of the matrix system. It is important to point out that the solution of any BEM approach could also be substantially improved with the use of indirect solvers which were not considered in this work.

Only a few works have been reported in the literature on the BEM numerical solution of inelastic non-Newtonian flows. Phan Thien (1995) proposed a BEM solution of the non-homogeneous momentum equations based on the particular solution approach and RBF interpolation for the non-linear terms. Davis (1995) used the pseudo-body force technique and cell integration to model polymers and optimize mixing equipment. Davies also pointed out that the application of the DRM to the whole domain does not produce accurate results especially when there are high viscosity gradients.

The cell-integration BEM combined with subdomain techniques such as the Green's element method (GEM) (Taigbenu, 1995) have been applied together with a velocity-vorticity formulation by Skerget and Samec (1999), to model non-Newtonian flows in enclosures. As in other previous works by Skerget and collaborators (Skerget and Hribersek, 1996) for the Navier-Stokes equations, the integral formulation keeps the domain integrals without any further simplification. Also, Skerget and collaborators never considered the case of pressure boundary conditions which occurs very often in fluid dynamics processes and that can be easily handled by using a direct formulation in terms of velocity and tractions as the formulation presented here.

In the following sections, we will introduce the MD-DRM solution of the coupled system of Stokes equations and the energy equation for the non-Newtonian fluids with viscous dissipation effects. Besides the efficiency and accuracy of the proposed numerical method, the MD-DRM has the advantage of the robust RBF interpolation used in then DRM. Due to their smoothness or noise minimization character, the radial functions guarantee high accuracy on the evaluation of the gradient of the field variables (Hickernell, 1999). This property of the DRM interpolation permits a precise evaluation of the velocity and temperature derivatives directly from the solution of the matrix system without any additional burden.

The results obtained in this work suggest that the present multi-domain boundary element solution for non-isothermal and non-Newtonian problems is very accurate even for cases with strong viscosity gradients.

## 2. Governing equations

The system of mass, momentum and energy conservation equations for the steady state, non-isothermal flow of an incompressible fluid including buoyancy and viscous dissipation is given in tensor notation by

$$\frac{\partial u_i}{\partial x_i} = 0, \quad x \in \Omega \tag{1}$$

$$-\frac{\partial p}{\partial x_i} + \frac{\partial}{\partial x_j}(\eta \varepsilon_{ij}) + \rho g_i \beta (T - T_c) = 0, \quad x \in \Omega \tag{2}$$

$$k\frac{\partial^2 T}{\partial x_j \partial x_j} + \sigma_{ij}\varepsilon_{ij} = \rho C_p u_j \frac{\partial T}{\partial x_j}, \quad x \in \Omega \tag{3}$$

with boundary conditions

$$u_i = u_{i0}, \quad x \in \Gamma_u \tag{4}$$

$$t_i = \sigma_{ij} n_j = t_{i0}, \quad x \in \Gamma_t \tag{5}$$

$$T = T_0, \quad x \in \Gamma_T \tag{6}$$

$$q = -k\frac{\partial T}{\partial n} = q_0, \quad x \in \Gamma_q \tag{7}$$

where

$$\varepsilon_{ij} = \frac{1}{2}\left(\frac{\partial u_i}{\partial x_j} + \frac{\partial u_j}{\partial x_i}\right)$$

is the strain rate tensor; $\sigma_{ij}$ the total stress tensor; $u_i$ is the velocity vector; $t_i$ is the traction vector; $n_i$ is the outward unit normal to the boundary $\Gamma = \Gamma_u + \Gamma_t = \Gamma_T + \Gamma_q$ of the volume $\Omega$; $T$ is the fluid temperature at any point; $p$ the pressure and $q$ is the heat flux. In the above equations the classical summation convention has been used.

The thermophysical properties are: $\rho$ the fluid density, $\eta$ the viscosity which is a function of temperature and the generalized strain rate, $k$ is the thermal conductivity, $C_p$ the thermal capacity and $\beta$ is the coefficient of thermal expansion. The buoyancy force $\rho g_i \beta (T - T_c)$ in equation (2) represents the effect of temperature change on density, where $T_c$ is the reference temperature and $g_i$ is the magnitude of gravity acting in the $i$ direction. The term $\sigma_{ij}\varepsilon_{ij}$ in equation (3) is the irreversible rate of internal energy increase per unit volume by viscous dissipation or in other words the degradation of mechanical to thermal energy.

To convert this problem into a perturbation to a base Newtonian flow, the total stress tensor is decomposed into a Newtonian and a non-linear component as follows,

$$\sigma_{ij} = -p\delta_{ij} + \eta_{\mathrm{N}}\varepsilon_{ij} + \tau_{ij}^{(e)} \tag{8}$$

where $\eta_{\mathrm{N}}$ is an arbitrary constant viscosity that can be chosen to be the zero shear rate viscosity; and $\tau_{ij}^{(e)}$ represents the non-Newtonian effects in the stress tensor. For inelastic generalized Newtonian fluids the non-linear terms are:

$$\tau_{ij}^{(e)}(\dot{\gamma}) = (\eta - \eta_{\mathrm{N}})\varepsilon_{ij} \tag{9}$$

where the non-Newtonian viscosity $\eta$ is a function of the generalized shear rate $\dot{\gamma}$ given by

$$\dot{\gamma} = \sqrt{2\varepsilon_{ij}\varepsilon_{ji}} \tag{10}$$

With the formulation introduced in equation (8) the momentum equation (2) can be re-written as

$$-\frac{\partial p}{\partial x_i} + \eta_N \frac{\partial^2 u_i}{\partial x_j \partial x_j} + \rho g_i \beta(T - T_{\mathrm{c}}) + \frac{\partial \tau_{ij}^{(e)}}{\partial x_j} = 0 \tag{11}$$

The viscosity of most non-Newtonian fluids like polymers is usually a decreasing function of the generalized shear rate $\dot{\gamma}$ and this is known as shear-thinning behavior. For a Newtonian fluid the viscosity $\eta$ is a constant value $\mu$,

$$\eta(\dot{\gamma}) = \mu = \text{constant} \tag{12}$$

On the other hand, the most commonly used expression for the viscosity of a non-Newtonian fluid is the *Power-law* or *Ostwald-de-Waele* model (Agassant *et al.*, 1991),

$$\eta(\dot{\gamma}) = K\dot{\gamma}^{n-1} \tag{13}$$

where $K$ is called the consistency index and $n \in [0, 1]$, the power law index.

There are other more accurate semi-theoretical models to describe the behavior of non-Newtonian fluids, some of them are:

- The Carreau model (Agassant *et al.*, 1991)

$$\eta(\dot{\gamma}) = \eta_\infty + \frac{\eta_0 - \eta_\infty}{\left[1 + (\lambda\dot{\gamma})^2\right]^{(1-n)/2}} \tag{14}$$

  This model has four adjustable parameters to fit the experimental data: $\lambda$ is a characteristic time, $\eta_\infty$ is a constant viscosity at very high shear rates, $\eta_0$ and $n$ are the same as in the power law model.

- The hyperbolic tangent model (Agassant *et al.*, 1991)

$$\eta(\dot{\gamma}) = A - B\tanh\left(\frac{\dot{\gamma}}{k}\right)^{n} \tag{15}$$

where the parameters $A$, $B$, $k$ and $n$ are obtained by data fitting techniques to experimental data.

The above models account for the effect of the shear rate upon viscosity, however the actual viscosity is also dependent on temperature through the Andrade law (Agassant *et al.*, 1991; Osswald and Menges, 1995) of the form

$$\eta = \eta(\dot{\gamma})e^{\frac{E}{R}\left(\frac{1}{T}-\frac{1}{T_0}\right)} \tag{16}$$

where $E$ is the activation energy of the fluid; $R$ the ideal gas constant and $\eta(\dot{\gamma})$ is the viscosity evaluated at the reference temperature, $T_0$. Besides, in the above system of equations the flow field and temperature field are completely coupled, i.e. two way coupling, making the problem even more complex.

## 3. Multi-domain integral formulation

In the multi-domain BEM approach, the original domain is divided into smaller subregions or subdomains, each of them enclosed by a certain number of boundary elements. The solution of the partial differential equations (1)-(3) in each subdomain is given in terms of the corresponding integral representation formula. Also, adjacent domain-elements have to be matched according to some continuity or compatibility conditions for all the variables namely velocity, traction, temperature and heat flux.

From the integral representation of equation (11) given by Ladyzhenskaya (1963), it is found that the $i$ component of the velocity field at a point $x$ of the $n$th subregion bounded by the contour $\Gamma_n$ that encloses the sub-domain $\Omega_n$ is given by

$$c_{ik}u_i(x) = \int_{\Gamma_n} K_{kj}(x,y)u_j(y)\,d\Gamma_y - \int_{\Gamma_n} U_i^k(x,y)t_i^N(y)\,d\Gamma_y - \int_{\Omega_n} U_i^k(x,y)g_i(y)\,d\Omega_y \tag{17}$$

for $n = 1, 2, \ldots, M$, where $M$ is the total number of subregions.

In the above equations, $t_i^{\mathrm{N}}(y)$ is the $i$th component of the Newtonian based traction due to the flow field $(\vec{u}, p)$, i.e. $t_i^{\mathrm{N}}(y) = (-p\delta_{ij} + \eta_{\mathrm{N}}\varepsilon_{ij})n_j(y)$. The kernel $U_i^k(x,y)$ is the $i$th component of the velocity field of the fundamental solution of

the Newtonian Stokes system of equations (Stokeslet), located at the point $y$ and oriented in the $k$th direction,

$$U_i^k(x,y) = -\frac{1}{4\pi\eta_N}\left[\ln\left(\frac{1}{r}\right)\delta_{ik} + \frac{(x_i - y_i)(x_k - y_k)}{r^2}\right] \tag{18}$$

where $r$ is the distance from point $y$ to any other point $x$, i.e. $r = |x - y|$, and

$$\begin{aligned} K_{ik} &= \sigma'_{ij}\left(\vec{u}^k(x,y), q^k(x,y)\right)n_j(y) \\ &= \left(q^k(x,y)\delta_{ij} + \eta_N\left(\frac{\partial U_i^k(x,y)}{\partial x_j} + \frac{\partial U_k^i(x,y)}{\partial x_j}\right)\right)n_j(y) \\ &= -\frac{1}{\pi r}\frac{(x_i - y_i)(x_k - y_k)(x_j - y_j)}{r^3}n_j \end{aligned} \tag{19}$$

is the traction corresponding to the flow field $(\vec{u}^k(x,y), q^k(x,y))$. The coefficients $c_{ik}$ have values between $\delta_{ik}$ and 0, being equal to $(1/2)\delta_{ik}$ for smooth boundaries, and equal to $c_{ik} = \delta_{ik}$ for points inside the domain $\Omega_n$.

Similarly, the integral representation of the energy transport equation at each domain (equation (3)) can be obtained by applying Green's second theorem for a scalar function (Brebbia and Dominguez, 1992), and it is expressed as follows

$$cT(x) = \int_{\Gamma_n} H(x,y)T(y)\,d\Gamma_y - \int_{\Gamma_n} G(x,y)q(y)\,d\Gamma_y + \int_{\Omega_n} G(x,y)h(y)\,d\Omega_y \tag{20}$$

where

$$q(x) = k\frac{\partial T}{\partial n} \tag{21}$$

and $G$, $H$ are the fundamental solution and its normal derivative along the integration path, respectively, (Brebbia *et al.*, 1984), i.e.

$$G(x,y) = \frac{1}{2\pi k}\log r \tag{22}$$

and

$$H(x,y) = \frac{1}{2\pi}\frac{\partial \log r}{\partial n_y} \tag{23}$$

The domain integrals in expressions (17) and (20) account for all the non-linear terms in the original partial differential equations (11) and (3), i.e.

$$g_i = -\rho g_i \beta (T - T_c) - \frac{\partial \tau_{ij}^{(e)}}{\partial x_j} \tag{24}$$

$$h = u_j \frac{\partial T}{\partial x_j} - \sigma_{ij} \varepsilon_{ij} \tag{25}$$

The final set of equations is completed by assembling the integral equations (17) for each subdomain, using the traction equilibrium and velocity compatibility at the common interfaces between subregions, i.e. $u_i^{(+)} = u_i^{(-)}$ and $\sigma_{ij}^{(+)} n_j + \sigma_{ij}^{(-)} n_j = 0$. Likewise, the integral equations (20) must also be assembled using the continuity of the temperature field and the heat flux balance condition, i.e. $T_i^{(+)} = T_i^{(-)}$ and

$$\frac{\partial T^{(+)}}{\partial x_j} n_j + \frac{\partial T^{(-)}}{\partial x_j} n_j = 0.$$

The cell integration approach and the DRM are two possible alternatives to deal with the domain integral in equations (17) and (20) in each subregion. When cell integration is used to evaluate the domain integral in each subregion the GEM is recovered. On the other hand, if the domain integrals are converted into equivalent boundary integrals in each subdomain the method will be known as MD-DRM.

As explained in our earlier articles (Florez and Power, 2000; Florez *et al.*, 2000), dealing with different problems to the present one, the non-linear terms that appear within the domain integrals in equation (17) and (20) can be approximated using a series of particular solutions and interpolation functions. To express the domain integral in equation (17) in terms of equivalent boundary integrals, the DRM approximation is introduced. The basic idea is to expand the $\vec{g}(x)$ term using radial interpolation functions at each sub-region, i.e.

$$g_i(x) = \sum_{m=1}^{N+L+A} f^m(x) \alpha_l^m \delta_{il} \tag{26}$$

The coefficients $\alpha_l^m$ are unknowns to be determined by collocation on a set of $N$ nodes on the boundary and $L$ internal nodes. It will be considered here that there are $A=3$ augmentation global functions from the set $\{1, x_1, x_2\}$.

An augmented spline consists of a RBF plus a series of additional global functions (Goldberg and Chen, 1997). The RBF used in this work is the thin-plate spline:

$$f^m(x) = f(r(x, y^m) = r^2 \log r \quad m = 1, \ldots, N + L \tag{27}$$

where $r = |x - y^m|$ is the Euclidean distance between the field point, $x$ and the collocation point, $y^m$. Although many different RBFs are discussed by

Goldberg and Chen (1997), the thin plate spline has been successfully used before in this type of formulation that make it the recommended choice (Mingo and Power, 2000).

Equation (26) when applied to the $N+L$ collocation nodes will generate 2 ($N+L$) linear equations with 2 ($N+L+A$) unknowns and therefore $2A$ additional conditions are necessary which basically guarantee an optimum interpolant (Goldberg and Chen, 1997). These additional relationships are:

$$\sum_{j=1}^{N+L} \alpha_l^j \delta_{il} = \sum_{j=1}^{N+L} x_1^j \alpha_l^j \delta_{il} = \sum_{j=1}^{N+L} x_2^j \alpha_l^j \delta_{il} = 0 \tag{28}$$

where $x^j$ represents the $j$th collocation node.

Similarly, in the energy equation (20) the convective term can be approximated as:

$$h(x) = \sum_{m=1}^{N+L+A} f^m(x)\beta^m \tag{29}$$

Now, we define the auxiliary velocity field $\left(\hat{U}_i^{lm}(x), \hat{p}^{lm}(x)\right)$ (Power and Wrobel, 1995) which is a solution of the following equations:

$$\mu \frac{\partial^2 \hat{U}_i^{lm}(x)}{\partial x_j \partial x_j} - \frac{\partial \hat{p}^{lm}(x)}{\partial x_i} = f^m(x)\delta_{il} \tag{30}$$

$$\frac{\partial \hat{U}_i^{lm}}{\partial x_i} = 0 \tag{31}$$

and also the auxiliary thermal field, $\hat{T}$, which satisfies the following Poisson equation,

$$k \frac{\partial^2 \hat{T}^m(x)}{\partial x_j \partial x_j} = f^m(x) \tag{32}$$

At this point, we can apply Green's identities to both the auxiliary velocity field and the auxiliary thermal field to obtain integral representation formulae only in terms of boundary integrals (Florez and Power, 2000; Florez *et al.*, 2000; Partridge *et al.*, 1992; Power and Wrobel, 1995), thus

$$c_{kj}(x)u_k(x) - \int_{\Gamma_n} K_{kj}(x,y)u_j(y)\,\mathrm{d}\Gamma_y + \int_{\Gamma_n} U_i^k(x,y)t_j^N(y)\,\mathrm{d}\Gamma_y$$
$$= \sum_{m=1}^{N+L+A} \alpha_l^m \left\{ c_{kj}(x)\hat{U}_k^{lm}(x) - \int_{\Gamma_n} K_{kj}(x,y)\hat{U}_j^{lm}(y)\,\mathrm{d}\Gamma_y + \int_{\Gamma_n} U_i^k(x,y)\hat{t}_j^{lm}(y)\,\mathrm{d}\Gamma_y \right\} \tag{33}$$

$$cT(x) - \int_{\Gamma_n} H(x,y)T(y)\,\mathrm{d}\Gamma_y + \int_{\Gamma_n} G(x,y)q(y)\,\mathrm{d}\Gamma_y$$
$$= \sum_{m=1}^{N+L+A} \beta^m \left\{ c\hat{T}^m(x) - \int_{\Gamma_n} H(x,y)\hat{T}^m(y)\,\mathrm{d}\Gamma_y + \int_{\Gamma_n} G(x,y)\hat{q}^m(y)\,\mathrm{d}\Gamma_y \right\} \tag{34}$$

where $\hat{q}^m = \partial \hat{T}^m/\partial n$. The particular solution of equations (31), (30) and (32) have been obtained by Florez and Power (2001a) and Mingo and Power (2000) and are presented in the appendix.

## 4. Approximation of derivatives

The evaluation of the extra stress tensor, $\tau_{ij}^{(e)}$, and other terms appearing in equations (24) and (25), requires the numerical approximation of derivatives of velocity and temperature. Once these derivatives are known, they can be used to obtain the value of the non-Newtonian viscosity, the stress tensor and the convective terms at each point of each subdomain.

If the nodal velocities and temperatures are approximated using augmented thin plate splines, i.e.

$$u_i(x) = \sum_{m=1}^{N+P} f^m(x)\beta_l^m\,\delta_{il} \tag{35}$$

$$T = \sum_{m=1}^{N+L+A} f^m(x)\gamma^m \tag{36}$$

or equivalently in matrix notation,

$$\mathbf{u} = \mathbf{F}\boldsymbol{\beta} \tag{37}$$

$$\mathbf{T} = \mathbf{F}\boldsymbol{\gamma} \tag{38}$$

then the derivatives can be readily obtained by the differentiation of equations (37) and (38),

$$\frac{\partial u_i(x)}{\partial x_j} = \sum_{m=1}^{N+P} \frac{\partial f^m(x)}{\partial x_j} \beta_l^m \, \delta_{il} \tag{39}$$

$$\frac{\partial T}{\partial x_j} = \sum_{m=1}^{N+L+A} \frac{\partial f^m(x)}{\partial x_j} \gamma^m \tag{40}$$

or in a more compact matrix notation,

$$\frac{\partial \mathbf{u}}{\partial x_j} = \frac{\partial \mathbf{F}}{\partial x_j} \boldsymbol{\beta} \tag{41}$$

$$\frac{\partial \mathbf{T}}{\partial x_j} = \frac{\partial \mathbf{F}}{\partial x_j} \boldsymbol{\gamma} \tag{42}$$

Inverting equations (37) and (38) and substituting the results into (41) and (42) we obtain the following expressions:

$$\frac{\partial \mathbf{u}}{\partial x_j} = \frac{\partial \mathbf{F}}{\partial x_j} \mathbf{F}^{-1} \mathbf{u} \tag{43}$$

$$\frac{\partial \mathbf{T}}{\partial x_j} = \frac{\partial \mathbf{F}}{\partial x_j} \mathbf{F}^{-1} \mathbf{T} \tag{44}$$

where the matrix $\partial \mathbf{F}/\partial x_j$ contains the derivatives of the interpolation functions with respect to $x_j$, $\mathbf{u}$ is the vector of velocities at the collocation nodes and $\mathbf{T}$ is the vector of temperatures at the nodes. The robustness of the above approximation for the gradient is guaranteed by the smoothness property of the RBF (Hickernell, 1999).

## 5. Discretization of the integral equations

For the numerical solution of the problem, the surface $\Gamma_n$ of each subdomain can be discretised by means of isoparametric linear boundary elements. Along each element the integrals are calculated in terms of the nodal values of the velocity and tractions and using linear interpolation functions. In this way, Equations (33) and (34) can be written in matrix form as:

$$(c\mathbf{u})_i - \mathbf{K}_{ik}\mathbf{u}_k + \mathbf{L}_{ik}\mathbf{t}_k^N = \sum_{m=1}^{N+P} \alpha_j (\mathbf{K}_{ik}\hat{\mathbf{t}}_{kj} - \mathbf{L}_{ik}\hat{\mathbf{u}}_{kj} + (c\hat{\mathbf{u}}_{ij})) \tag{45}$$

$$(c\mathbf{T})_i - \mathbf{H}_{ik}\mathbf{T}_k + \mathbf{G}_{ik}\mathbf{q}_k = \sum_{m=1}^{N+P} \beta_j(\mathbf{H}_{ik}\hat{\mathbf{T}}_{kj} - \mathbf{G}_{ik}\hat{\mathbf{q}}_{kj} + (c\hat{\mathbf{T}})_j) \tag{46}$$

where $\mathbf{H}_{ik}$, $\mathbf{G}_{ik}$, $\mathbf{K}_{ik}$ and $\mathbf{L}_{ik}$ are the standard influence matrices resulting from the integrations over the boundary elements, the index $i$ represents de collocation nodes, $k$ the nodes at the integration elements and $j$ the DRM collocation points. In the present case, these matrices result from the integration over the four elements that form each subdomain.

To find the value of the coefficients, $\alpha_l^m$ and $\beta_j$, in equations (45) and (46), equations (26) and (29) is applied at each of the $N+L$ chosen collocation nodes of each subdomain, boundary and internal, and imposes simultaneously the orthogonality conditions to complete the terms of the polynomials. In this way, the following systems of equations are obtained,

$$\mathbf{F}\boldsymbol{\alpha} = \mathbf{g} \tag{47}$$

$$\mathbf{F}\boldsymbol{\beta} = \mathbf{h} \tag{48}$$

that can be inverted to get the values of the unknown coefficients, i.e.

$$\boldsymbol{\alpha} = \mathbf{F}^{-1}\mathbf{g} \tag{49}$$

$$\boldsymbol{\beta} = \mathbf{F}^{-1}\mathbf{h} \tag{50}$$

Micchelli (1986) proved that for a case when the nodal points are all distinct, the matrix resulting from any of the RBF interpolation given before is always non- singular.

When the discrete integral equations for each domain-element equations (45) and (46) are put together, the final systems of equations are written in matrix notation as,

$$\mathbf{K}\mathbf{u} - \mathbf{L}\mathbf{t} = -(\mathbf{K}\hat{\mathbf{u}} - \mathbf{L}\hat{\mathbf{t}})\boldsymbol{\alpha} \tag{51}$$

$$\mathbf{H}\mathbf{u} - \mathbf{G}\mathbf{q} = -(\mathbf{H}\hat{\mathbf{u}} - \mathbf{G}\hat{\mathbf{t}})\boldsymbol{\beta} \tag{52}$$

As explained in Sections 3 and 4 the unknown coefficients, $\boldsymbol{\alpha}$ and $\boldsymbol{\beta}$, are determined by collocation on the boundary nodes of each subdomain (Florez and Power, 2001b). According to the approximations explained in Section 4, the vector $\boldsymbol{\alpha}$ is expressed in terms of velocities and temperatures at the collocation nodes, and vector $\boldsymbol{\beta}$ can be expressed in terms of nodal temperatures only. Therefore, both equations (51) and (52) are non-linear systems and also are coupled through several temperature terms. Each system of equations (51) and (52) for the entire domain can be solved using the Newton-Raphson scheme

combined with a line-search algorithm intended to reduce the error at each iteration (Dennis and Schnabel, 1980).

To account for the coupling between the momentum and energy equations, we used direct iteration. The velocity in the convective term from the energy equation is considered as a known variable from the previous solution of the momentum equations obtained by the Newton-Raphson method. Likewise, at each iteration the temperature-dependent terms in the momentum equations can be known from the previous solution of the energy equation.

For fluids with variable viscosity, there is an additional source of problems in the numerical iteration. In the multi-domain solution of non-Newtonian problems there will be sub-domains where the viscosity remains nearly constant and other regions with higher gradients where the viscosity changes ostensibly. These differences between sub-regions can make the residual function of the iterative method have flat regions of local minima or valleys where the iteration process stagnates. Additionally, the dual reciprocity method for the non-Newtonian case is based in a perturbation formulation given in equation (11), so when the assumed constant viscosity $\eta_N$ is very far from its actual value $\eta$, Newton's method might not make good progress unless the initial guess for the iterations is very close to the true solution. To alleviate the problems mentioned above, a predictor-corrector approach was designed in which a sequence of linear problems can be solved to get a better initial guess for starting the non-linear iterations. In the predictor stage each sub-domain is assumed to have a constant viscosity equal to the average viscosity of the boundary nodes that define the subdomain. This average value is then corrected in the corrector stage of the process when the original non-linear system of equations is solved by Newton's method until convergence is reached. If Newton's method stops at a local minimum, the predictor step can be performed once again, but starting from that local minimum and so on.

## 6. Numerical examples

Three different non-isothermal problems with viscous dissipation were solved using the MD-DRM approach. The results show the ability of the multidomain method to model complex non-isothermal and non-Newtonian flows with viscous dissipation effects.

### *6.1 Non-Newtonian slit flow with viscous dissipation*

Let us consider the flow of a non-Newtonian fluid between two parallel plates (planar poiseuille flow) with a constant wall temperature equal to $T_0$, the initial temperature of the fluid, inlet temperature, $T_0$ and zero temperature longitudinal gradient at the outlet. The flow is assumed fully developed, at a Reynolds number, $\mathrm{Re} \ll 1$, and one-dimensional along the $x$-axis with negligible variations of the viscosity with temperature, i.e. one way coupling. Buoyancy effects due to temperature differences have also been neglected. The flow

between the plates is caused by a pressure drop $\Delta p = p_1 - p_2 = 300\,\text{Pa}$ between the ends of the channel. The length of the channel is $L = 15\,\text{m}$ and the width $h = 1\,\text{m}$. Figure 1 shows the uniform mesh of $40 \times 20$ subdomains used for the MD-DRM solution of the slit flow problem.

The governing equations for this problem including the viscous dissipation term $\sigma_{ij}\varepsilon_{ij}$, are: the mass conservation equation, equation (1), the momentum equation, equation (2) with $\beta = 0$, and the energy equation, equation (3), with the constitutive equations:

$$\sigma_{ij} = -p\,\delta_{ij} + \eta\varepsilon_{ij}; \quad \eta = K\dot{\gamma}^{n-1} \tag{53}$$

Figure 2 shows the obtained velocity profile for different values of the power law index $n$, as well as a comparison of the obtained results with the known analytical solution. As can be observed they are in good agreement, even that in our solution we only used uniform distribution of subdomains. It is important to observe that when using uniform distribution of subdomains, due to the geometric similarity and the characteristic of the kernels used in our

**Note:** For the numerical solution of the slit flow problem

**Figure 1.**
$40 \times 20$ subdomains mesh

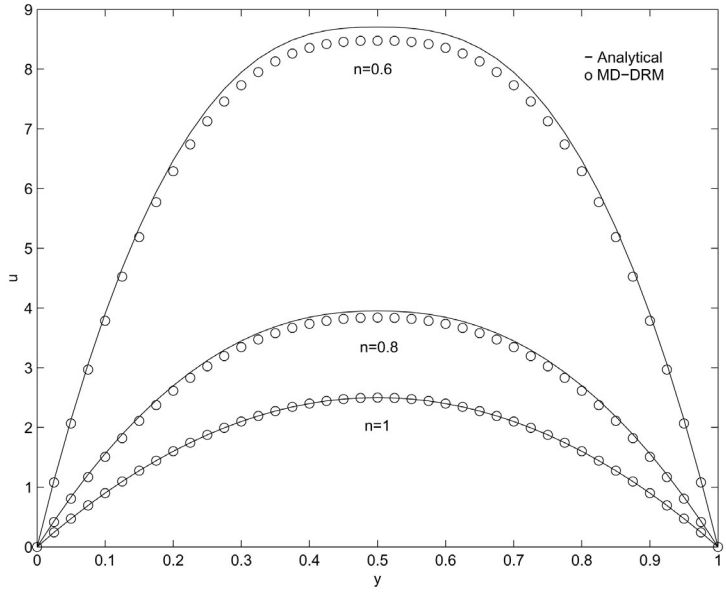


**Figure 2.**
Velocity profile for the slit flow problem with viscous dissipation for different values of the power law index $n$

integral equation formulation, the numerical evaluation of the matrices in each subdomain need to be carried out only in one of the subdomains.

The temperature variation along the channel shows three distinguished zones.

(1) Near the entrance of the channel the temperature rise is small and the heat conduction through the wall is negligible. Most of the power dissipated is used to heat the fluid, as if the liquid was thermally insulated from the surroundings. This is called the *adiabatic regime*.

(2) Somewhere downstream from the entrance the temperature rise is higher and conduction can no be longer neglected. This zone is called the *transition regime* in which both energy conduction and advection are important.

(3) Further downstream, the temperature reaches a limiting value and all the dissipated power is transferred by conduction to the surroundings. This is the *equilibrium regime*.

Figure 3 shows the temperature profile in the equilibrium regime for a power law fluid at different values of the power law index, $n$. In this figure, the numerical results have been compared to the analytical solution given by Agassant *et al.* (1991), and the error percentage is always less than 3.5 percent.

Figure 4, shows the comparison between our estimation of the viscosity profile for different values of the power law index, $n$ and those obtained with the corresponding analytical solution showing as before excellent agreement.

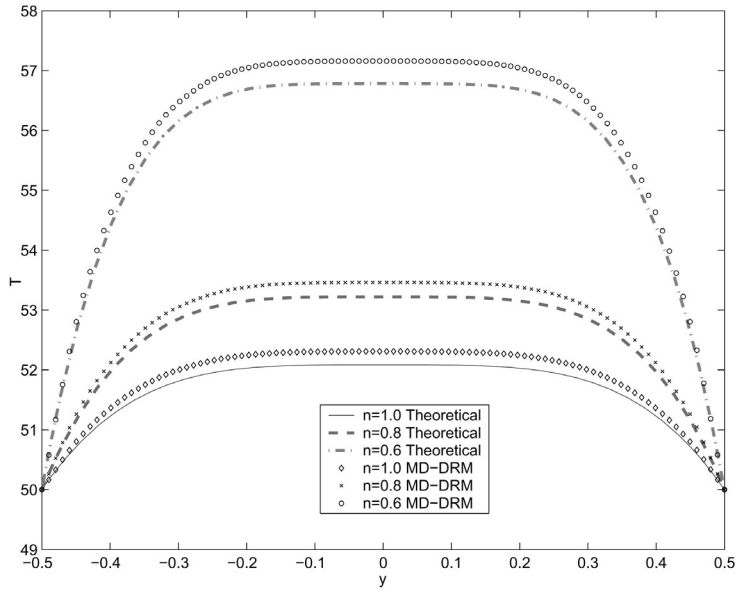


**Figure 3.**
Temperature profiles for different values of the power law index $n$ including viscous dissipation effects

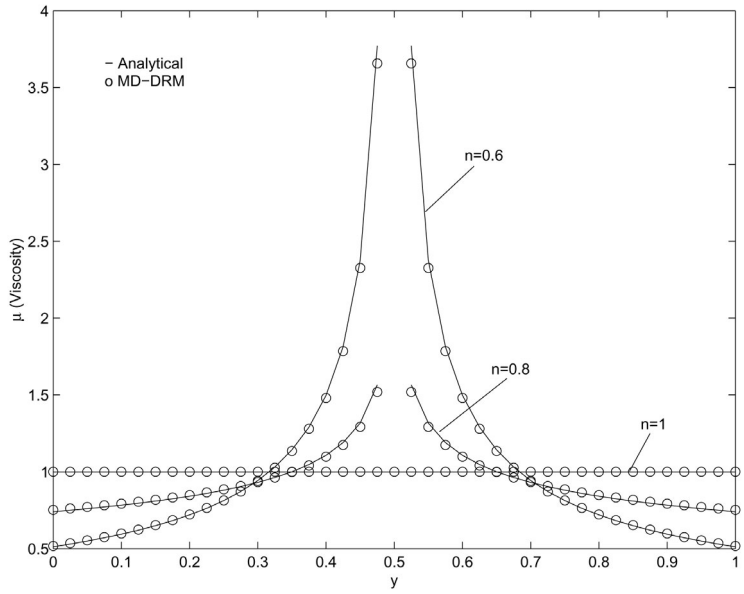


**Figure 4.**
Viscosity profiles for the slit flow problem with viscous dissipation at several values of the power law index, $n$

All the simulations presented here were run in a COMPAQ Pentium II desktop with 400 MHz, and not more than ten iterations were necessary before convergence was attained. The convergence criteria used in this work was defined as

$$\frac{\|u_{\text{new}} - u_{\text{old}}\|}{\|u_{\text{new}}\|} \leq 10^{-6} \tag{54}$$

for the momentum equations and

$$\frac{\|T_{\text{new}} - T_{\text{old}}\|}{\|T_{\text{new}}\|} \leq 10^{-6} \tag{55}$$

for the temperature field.

*6.2 Non-isothermal Couette flow with viscous dissipation*

In this example, we consider the flow of an incompressible power-law fluid between the two axial cylinders as shown in Figure 5. As the inner cylinder rotates, each cell of fluid rubs against the adjacent cells. This rubbing of adjacent layers of fluid produces heat; that is, mechanical energy is degraded into thermal energy. The magnitude of the viscous dissipation effect depends upon the local velocity gradient. The surfaces of the inner and outer cylinders are maintained at the same temperature, $T = T_0$. The geometry is defined by the radius, $R_1 = 1$ m and $R_2 = 5$ m.

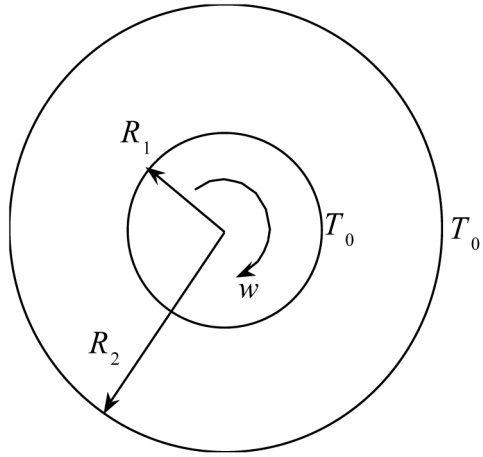


**Figure 5.**
Schematic representation of concentric cylinders for the Couette flow

For the MD-DRM numerical solution, a 400 subdomains mesh was used and it is shown in Figure 6. The mathematical model for this example is defined by the same governing equations than the previous example. However, here we will consider three different possibilities depending on whether the viscosity is dependent on temperature, on shear rate or on both. In all these cases the problem consists of a two way coupling system of non-linear equations.

*6.2.1 Case I. Viscosity does not vary with temperature* $\eta = \eta(\dot{\gamma})$. For a power-law fluid with a viscosity that is only a function of the generalized shear rate the rheological model is given by equation (13) in terms of the two constants, $K = 1\,\mathrm{Pa\,s}^n$ (the consistency coefficient) and $n$ (power law index), i.e. in this problem the viscosity does not change with the temperature. The numerical results for different values of the parameter $n$ can be seen in Figures 7-9.

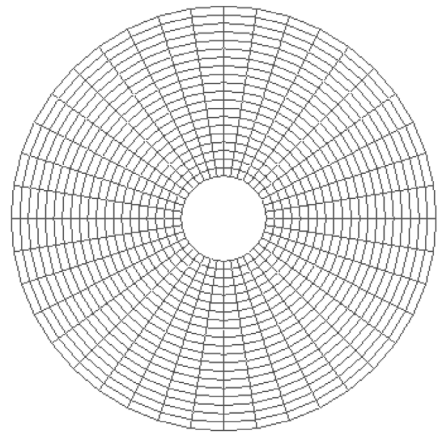

**Figure 6.**
$20 \times 20$ subdomains mesh used for MD-DRM solution of the Couette problem

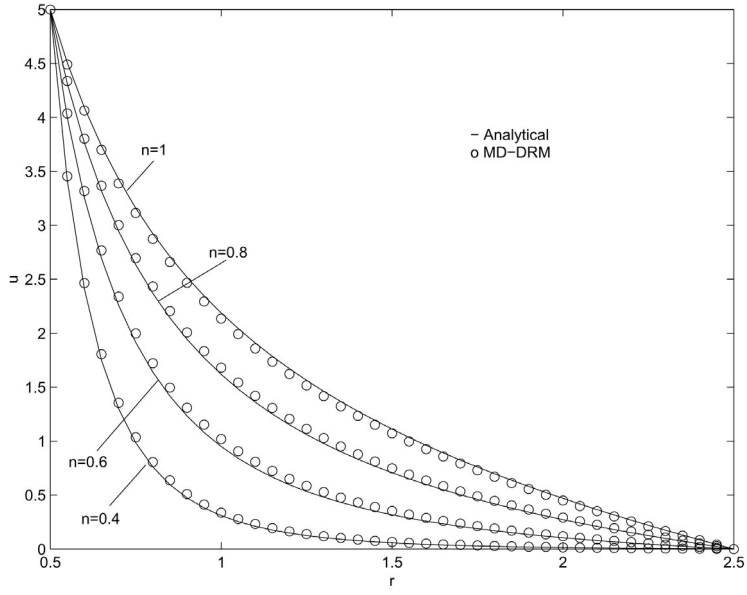


**Figure 7.**
Velocity profiles for the Couette flow problem with viscous dissipation

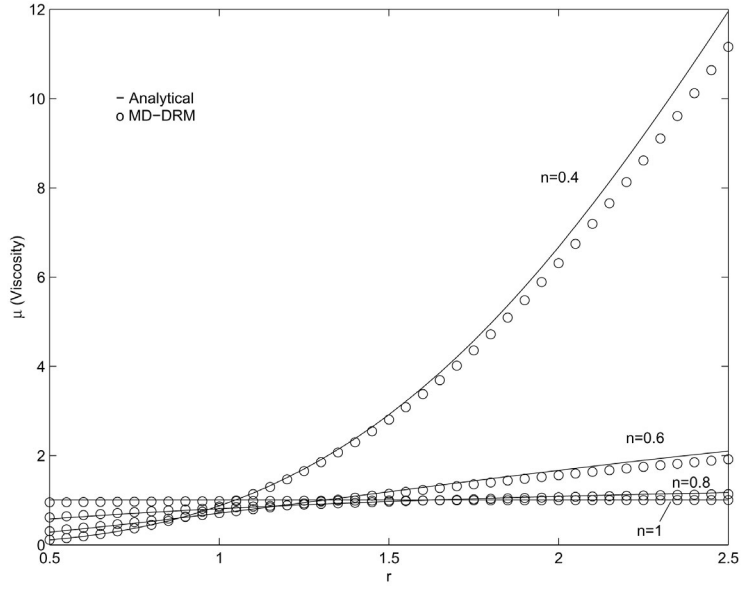


**Figure 8.**
Viscosity profiles for the Couette flow problem with viscous dissipation

Figure 7 shows the result for the different velocity profiles, Figure 8 the viscosity profiles and Figure 9 the temperature profiles. These results have been compared with the analytical solution obtained according to Bird *et al.* (1960) by direct integration of the momentum and energy equations. In all the

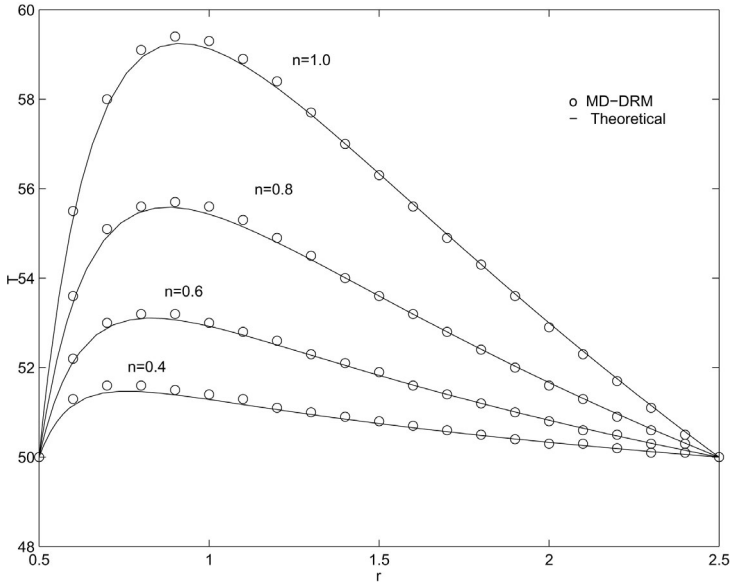


**Figure 9.**
Temperature profiles for the Couette flow problem with viscous dissipation

cases, the numerical error was less than 0.5 percent, as shown in the figures. It is important to point out that the circular geometry was approximated by linear elements. Better results are expected with the use of quadratic boundary elements, which exactly represent the geometric.

*6.2.2 Case II. Viscosity is a function of temperature only* $\eta = \eta(\mathrm{T})$. In this case we have considered that viscosity is constant (Newtonian fluid) and the temperature rise in the fluid results in variations of the viscosity which then affect the velocity profile. The equations of motion and energy are coupled and must be solved by an iterative method for each point of the flow system. The expression for the viscosity in this case is the following (see equation (16))

$$\eta = \eta_0 e^{\frac{E}{R}\left(\frac{1}{T}-\frac{1}{T_0}\right)} \tag{56}$$

with $\eta_0 = 1\,\mathrm{Pa\,s}$.

In Figures 10-12, we show the comparison between our numerical solution for different values of the activity energy coefficient $\Xi$ and the solution obtained with a complete different numerical scheme for the velocity, temperature and viscosity profiles, respectively. As before the agreement between the two solutions is excellent. The numerical scheme used to validate our result was based upon a finite difference 3-stage Lobatto IIIa formula which is basically a collocation technique (Shampine, 1994).

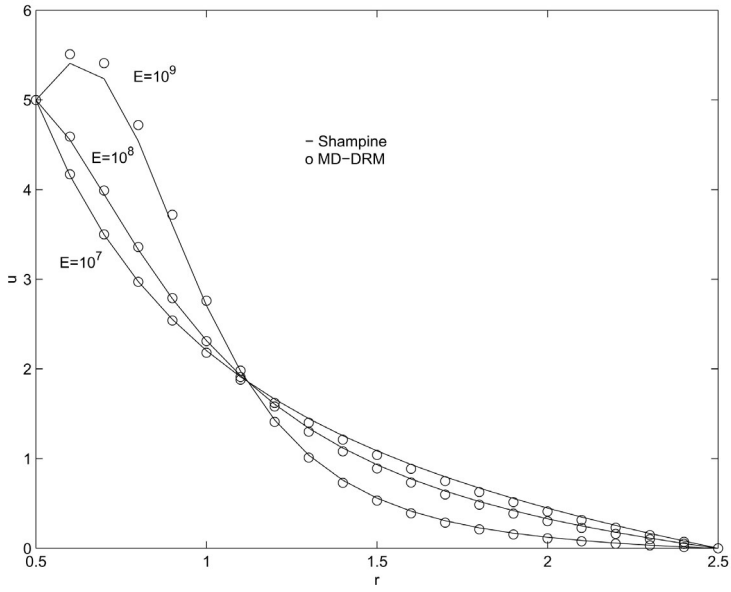


**Figure 10.**
Velocity profiles for the Couette flow problem with temperature dependent viscosity

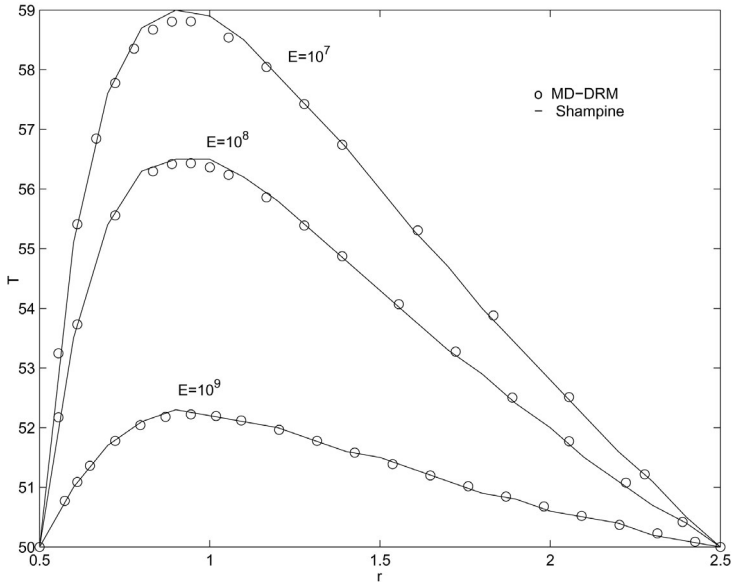


**Figure 11.**
Temperature profiles for the Couette flow problem with a temperature dependent viscosity

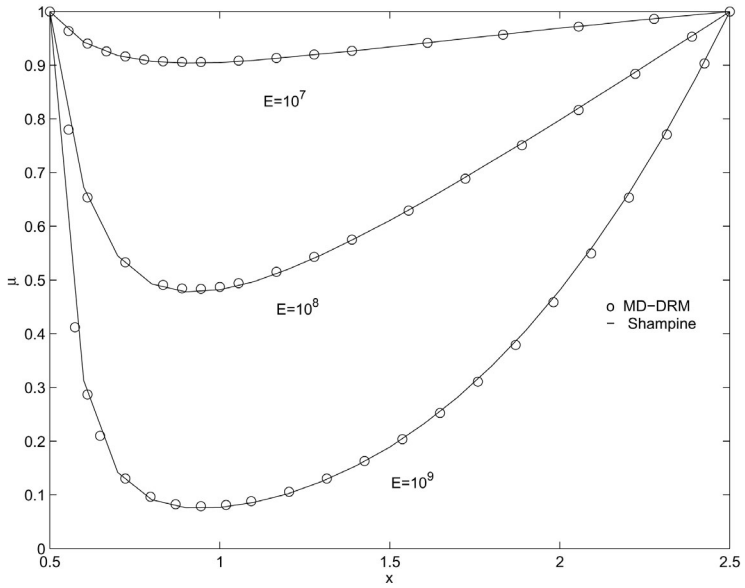


**Figure 12.**
Viscosity profiles for the Couette flow problem with temperature dependent viscosity

*6.2.3 Case III. Viscosity is a function of both, shear rate and temperature* $\eta = \eta(\dot{\gamma}, \mathrm{T})$. This is the most complex case where the effects of shear rate and temperature affect the value of viscosity, i.e.

$$\eta = K\dot{\gamma}^{n-1} e^{\frac{E}{R}\left(\frac{1}{T}-\frac{1}{T_0}\right)}. \tag{57}$$

As before, in this case we compare our results with those obtained with the FDM mentioned above (Shampine, 1994).

Figures 13-15 show the comparison between the velocity, temperature and viscosity profiles obtained with the two approaches. The numerical results were obtained for two different values of the power law index, $n$ of a non-Newtonian fluid at a constant activation energy, $E = 10^7$ J/mol, and as can be seen on these figures the MD-DRM results are very close to the test solution with a numerical difference less than 1 percent.

*6.3 Natural convection with viscous dissipation in a vertical channel*

In this final example, natural convection in a parallel-plate vertical channel of a Newtonian fluid is analyzed in the fully developed region by considering the effect of viscous dissipation. Figure 16 shows a schematic of the problem. The two boundaries are considered as isothermal and kept either at equal or at different temperatures. Many analyses of convection flow in a parallel-plate vertical channel are available in the literature. A comprehensive review of the literature on this subject can be found in the work of Barletta (1998, 1999). Most

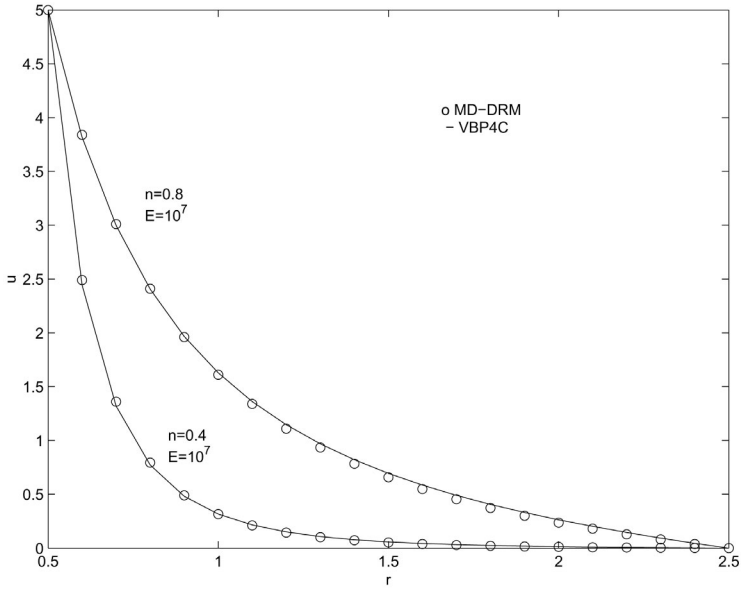


**Figure 13.**
Velocity profiles for the Couette flow problem with viscous dissipation and temperature dependent viscosity

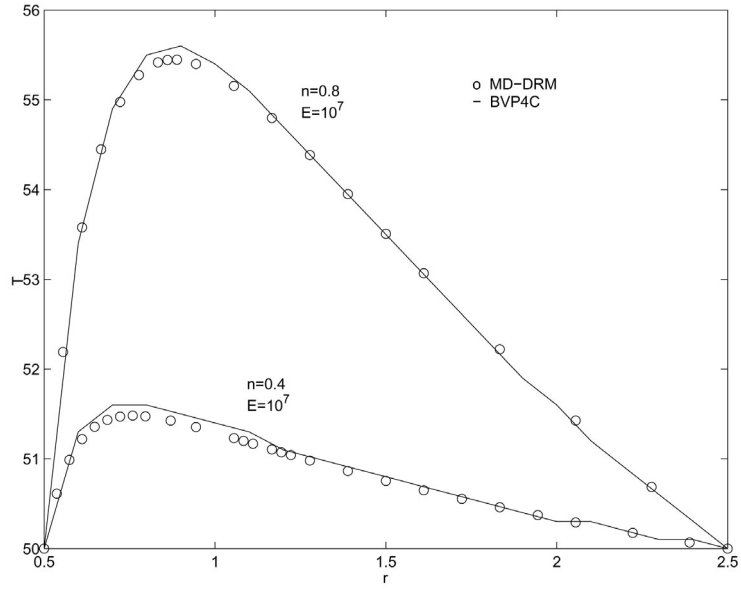


**Figure 14.**
Temperature profiles for the Couette flow problem with viscous dissipation and temperature dependent viscosity

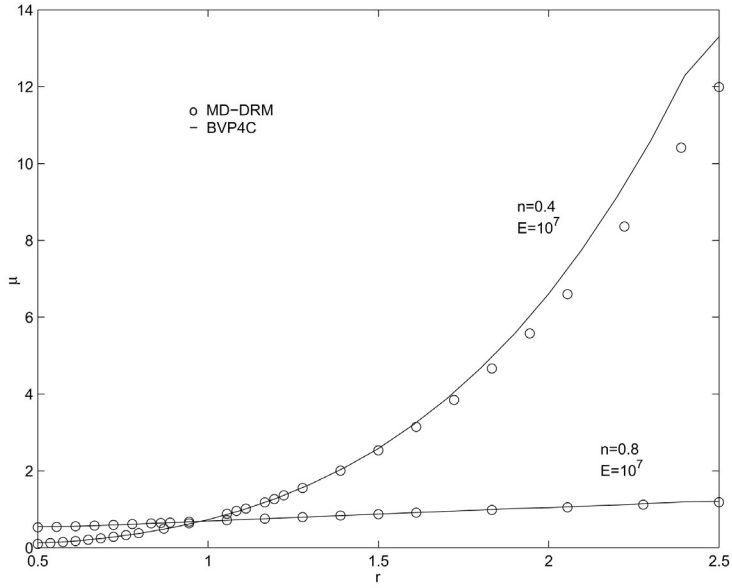


**Figure 15.**
Viscosity profiles for the Couette flow problem with viscous dissipation and temperature dependent viscosity

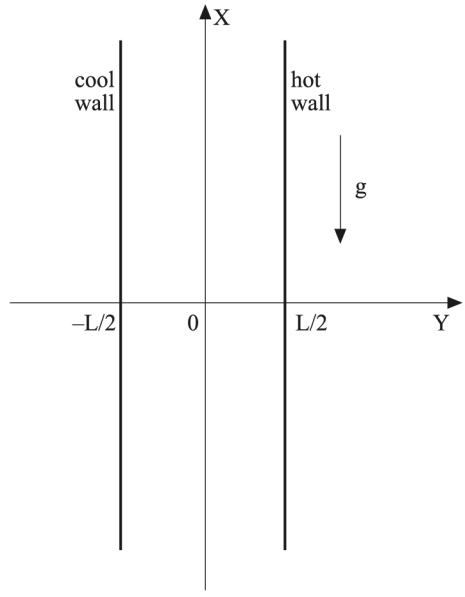


**Figure 16.**
Schematic representation of convective flow between parallel plates

of these studies present analytical and numerical solutions for the temperature and velocity field for prescribed wall temperatures, in particular, the work by Barletta (1998) is very special because he extended previous studies on laminar convection by considering the viscous dissipation effect. This effect is expected to be relevant for fluids with high values of the dynamic viscosity as well as for high-velocity flows. Indeed, when viscous dissipation cannot be neglected, the temperature field is dependent on the velocity field through a non-linear term in the energy balance equation.

The governing equations for the problem are: the mass balance equation,

$$\frac{\partial u_i}{\partial x_i} = 0 \tag{58}$$

the momentum balance equations

$$-\frac{\partial p}{\partial x_i} + \eta \frac{\partial^2 u_i}{\partial x_j \partial x_j} + \beta g_i (T - T_0) = 0 \tag{59}$$

and the energy equation,

$$k \frac{\partial^2 T}{\partial x_j \partial x_j} + \sigma_{ij} \varepsilon_{ij} = 0 \tag{60}$$

In all the above equations, the fluid is considered Newtonian with constant thermophysical properties. The temperature effect in the momentum equation has been taking in terms of the Boussinesq approximation, in this way by taking the dissipation and buoyancy effects a two way coupling problem is obtained.

For the problem depicted in Figure 16, the velocity and temperature profile can be obtained analytically by a perturbation method explained by Barletta (1998). This analytical solution was used to validate our numerical results obtained by the MD-DRM method.

The numerical results including both effects, i.e. natural convection and viscous dissipation, are given in terms of the following dimensionless parameters:

$$\begin{aligned} \mathrm{Gr} &= \frac{g\beta \Delta T D^3 \rho^2}{\eta^2}, \quad \Xi = \frac{\mathrm{Gr}}{\mathrm{Re}} \\ \mathrm{Re} &= \frac{\mathrm{U}_0 D \rho}{\eta}, \quad \mathrm{Pr} = \frac{\eta c_p}{k}, \quad \mathrm{Br} = \frac{\eta \mathrm{U}_0^2}{k \Delta T}, \end{aligned} \tag{61}$$

where

$$U_0 = -\frac{\frac{dP}{dx}D^2}{48\eta}, \quad T_0 = \frac{T_1 + T_2}{2} \tag{62}$$

with $D = 2L$. The perturbation solution found by Barletta was based upon the parameter $\varepsilon = \mathrm{Br}\Xi$.

For symmetric heating, i.e. $T_1 = T_2$, and when viscous dissipation is negligible, the temperature is uniform and no heat transfer occurs. In this case with an arbitrary value of $\Xi$ the usual Hagen-Poiseuille velocity profile is found. Figure 17 shows the obtained velocity profile with the MD-DRM approach for this case. Similar results are obtained for asymmetric heating with negligible buoyancy forces and relevant viscous dissipation. In this case, the parameter $\Xi$ is equal to zero.

In Figure 18, we present the obtained velocity profile for the case of $\mathrm{Br} = 0$, i.e. the temperature is transferred by pure conduction from asymmetric heating (no viscous dissipation), with values of $\Xi = 0$, 200 and 400. As expected for large values of $\Xi$ a reversal flow near the cool wall is observed.

On the other hand, Figure 19 shows the variation across the channel of the temperature for asymmetric heating in the case of $\Xi = 0$, i.e. purely forced convection occurs, with different values of $\mathrm{Br} = 0, 2$ and 4. In this case, as in the case of symmetric heating, Hagen-Poiseuille velocity profile is obtained (Figure 17). Although the conduction region holds only for $\mathrm{Br} = 0$, there is a region around the centre of the channel where the temperature is almost linear.

Finally, Figures 20 and 21, display the velocity and temperature profiles for the case of $\Xi = 500$ and values of $\varepsilon = 0$, 8 and 12 , i.e. both buoyancy and

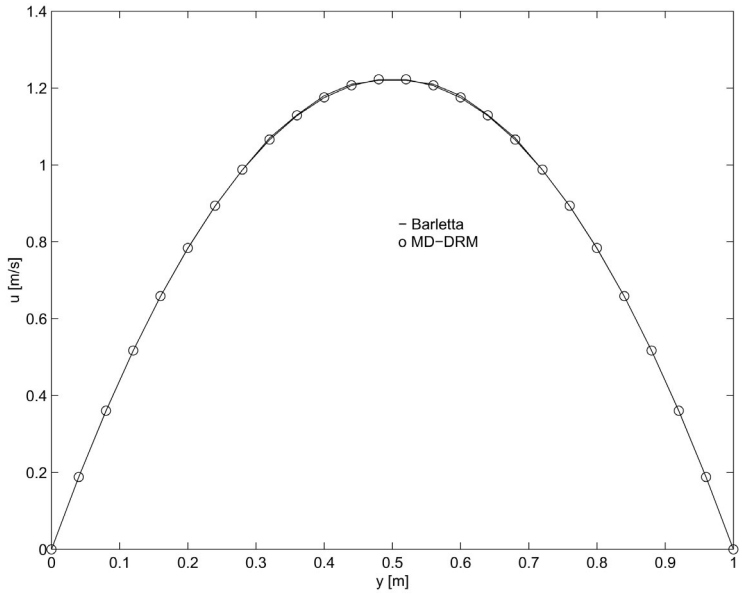


**Figure 17.**
Velocity variation along the channel width in the case of symmetric heating, for arbitrary values of $\Xi$, and the case of asymmetric heating with $\Xi = 0$

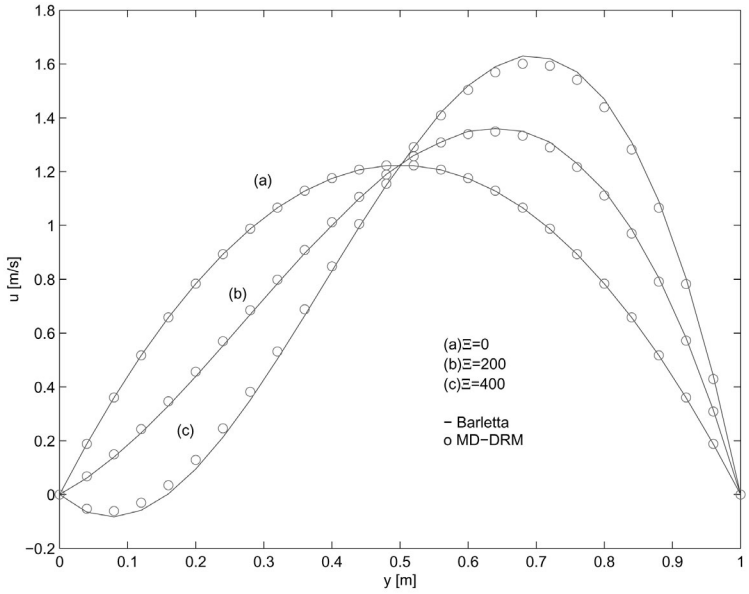


**Figure 18.**
Velocity variation along the channel width in the case of asymmetric heating, for different values of $\Xi$ and $Br = 0$

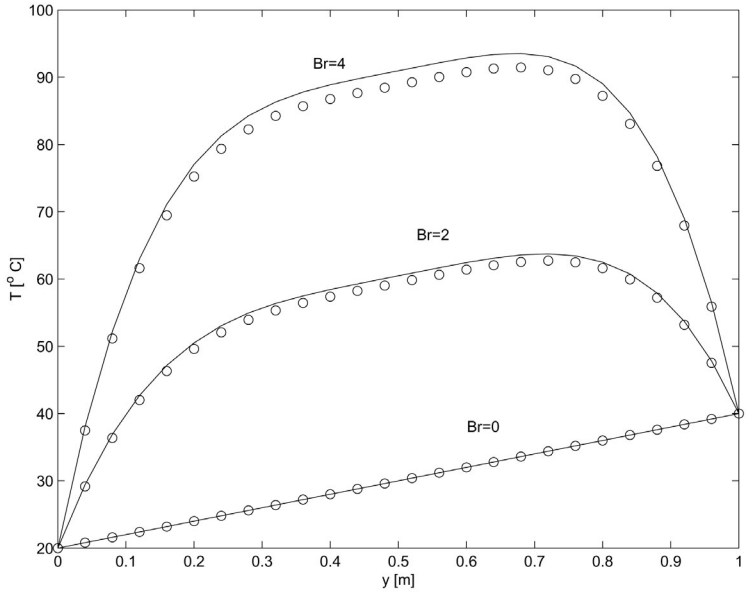


**Figure 19.**
Temperature variation along the channel width in the case of asymmetric heating, for different values of $Br$ and $\Xi = 0$

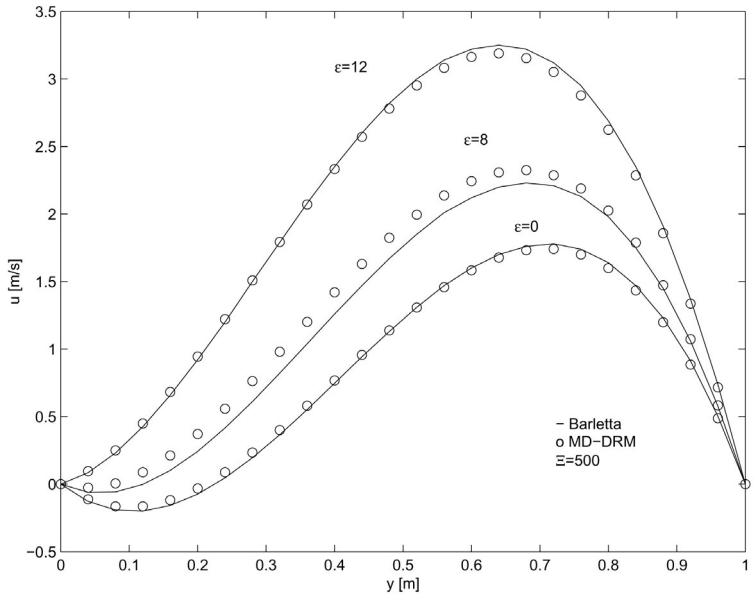


**Figure 20.**
Velocity variation along the channel width in the case of asymmetric heating, for different values of $\varepsilon$ and $\Xi = 500$

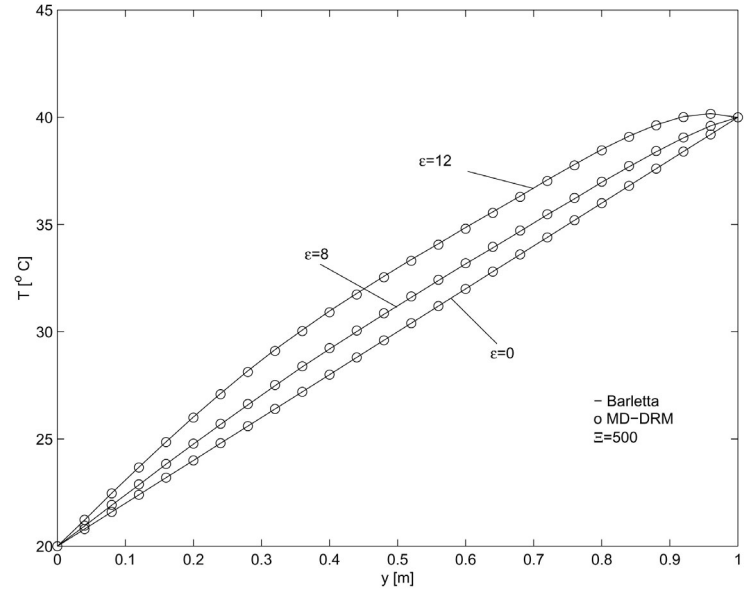


**Figure 21.**
Temperature variation along the channel width in the case of asymmetric heating, for different values of $\varepsilon$ and $\Xi = 500$

convection effects are present. For small values of $\varepsilon$, flow reversal close to the cool wall is present, while for large value of $\varepsilon$, no flow reversal appears. In this last case, viscous dissipation tends to increase the buoyancy force at each position and, as a consequence, it tends to contrast the flow reversal at the cool wall. In all these cases, the numerical solution obtained by the proposed MD-DRM is very close to the analytical solutions given by Barletta (1998).

## 7. Conclusion

In this work, a MD-DRM has been described and applied for the first time to the solution of non-isothermal non-Newtonian flow problems with viscous dissipation. The multi-domain technique is basically a domain partition method in which dives the entire domain into smaller regions. In each subregion or domain cell the integral representation formulae for the flow and temperature field are applied, and between adjacent regions the corresponding matching or continuity conditions are imposed. The domain integrals in each subdomain are treated by the DRM approximation in terms of one of the most efficient interpolation functions available in the mathematical literature. Despite the relatively rough meshes used and most simple boundary elements the results show convergence and high accuracy. For the number of subdomains used in this work, the accuracy of the solution decreases as the power index of the non-Newtonian fluid decreases due to the increase in the non-linear behaviour of the problem. In such cases, the accuracy can be improved by increasing the number of subdomains at the expense of additional computational cost.

Despite MD-DRM there are internal elements and a mesh, it must not be regarded as a domain method because all the domain integrals are converted into equivalent boundary integrals in each cell or element. Therefore, the proposed multi-domain method preserves the boundary only character of the BEM.

The different test examples presented show the versatility and efficiency of the proposed numerical scheme for the solution of non-linear flow problems. In the present paper, we have also extended the capabilities of the MD-DRM to non-isothermal non-Newtonian problems that had not been solved before using the DRM.

### References

Agassant, J.F., Avenas, P., Sergent, J.Ph. and Carreau, P.J. (1991), *Polymer Processing: Principles and Modeling*, Hanser Publishers, New York.

Barletta, A. (1998), "Laminar mixed convection with viscous dissipation in a vertical channel", *Int. J. Heat Mass Transfer*, Vol. 41, pp. 3501-13.

Barletta, A. (1999), "Laminar convection in a vertical channel with viscous dissipation and bouyancy forces", *Int. Comm. Heat Mass Transfer*, Vol. 26, pp. 153-64.

Bird, R.B., Stewart, W. and Lightfoot, E.N. (1960), *Transport Phenomena*, Wiley, New York.

Brebbia, C.A. and Dominguez, J. (1992), *Boundary Elements an Introductory Course*, Computational Mechanics Publications, Southampton.

Brebbia, C.A., Telles, J. and Wrobel, L.C. (1984), *Boundary Element Techniques*, Springer Verlag, Berlin, New York.

Davis, B.A. (1995), "Investigation of non-linear flows in polymer mixing using the boundary integral method", PhD thesis, Department of Mechanical Engineering, University of Wisconsin-Madison.

Dennis, J.E. and Schnabel, R.B. (1980), *Numerical Methods for Unconstrained Optimization and Non-linear Equations*, Prentice Hall, New Jersey.

Florez, W.F. and Power, H. (2000), "Multi-domain dual reciprocity {BEM} approach for the Navier-Stokes system of equations", *Commun. Num. Meth. Eng.*, Vol. 16, pp. 671-81.

Florez, W.F. and Power, H. (2001a), "Comparison between continuous and discontinuous boundary elements in the multidomain dual reciprocity method for the solution of the Navier-Stokes equations", *Engineering Analysis with Boundary Elements*, Vol. 25, pp. 57-69.

Florez, W.F. and Power, H. (2001b), "Multi-domain dual reciprocity for the solution of inelastic non-Newtonian problems", *Computational Mechanics*, Vol. 27, pp. 396-411.

Florez, W.F., Power, H. and Chejne, F. (2000), "Conservative interpolation for the boundary integral solution of the Navier-Stokes equations", *Computational Mechanics*, Vol. 26, pp. 507-13.

Goldberg, M.A. and Chen, C.S. (1997), *Discrete Projection Methods for Integral Equations*, Computational Mechanics Publications, Southampton.

Hickernell, F. (1999), "Radial basis function approximation as smoothing splines", *Appl. Math. Comput.*, Vol. 102 No. 1, pp. 1-24.

Kansa, E.J. and Carlson, R.E. (1995), "Radial basis functions: a class of grip-free, scattered data approximations", *Computational Fluid Dynamics Journal*, Vol. 3 No. 4, pp. 479-96.

Ladyzhenskaya, O.A. (1963), *The Mathematical Theory of Viscous Incompressible Flow*, Gordon and Breach, New York.

Micchelli, C.A. (1986), "Interpolation of scattered data: distance matrices and conditionally positive definite functions", *Const. Approx.*, Vol. 2, pp. 11-22.

Mingo, R. and Power, H. (2000), "The {DRM} subdomain decomposition approach for two-dimensional thermal convection flow problems", *Engineering Analysis with Boundary Elements*, Vol. 24, pp. 121-7.

Nardini, D. and Brebbia, C.A. (1982), *A New Approach to Free Vibration Analysis Using Boundary Elements*, B.E.M. IV, Computational Mechanics Publications and Springer Verlag, Southampton, Berlin.

Osswald, T.A. and Menges, G. (1995), *Materials Science of Polymers for Engineers*, Hanser Publishers, Munich.

Partridge, P.W., Brebbia, C.A. and Wrobel, L.C. (1992), *The Dual Reciprocity Boundary Element Method*, Computational Mechanics Publications, Southampton.

Phan Thien, N. (1995), "Applications of Boundary Element Methods in Non-Newtonian Fluid Mechanics", *B.E. Applications in fluid mechanics*, Computational Mechanics Publications, Southampton.

Popov, V. and Power, H. (1999), "The {DRM}-{MD} integral equation method for the numerical solution of convection-diffusion equation", *Boundary Element Research in Europe*, Computational Mechanics Publications, Southampton.

Power, H. and Wrobel, L.C. (1995), *Boundary Integral Methods in Fluid Mechanics*, Computational Mechanics Publications, Southampton.

Shampine, L.F. (1994), *Numerical Solution of Ordinary Differential Equations*, Chapman Hall Mathematics.

Skerget, L. and Hribersek, M. (1996), "Iterative methods in solving Naviers-Stokes equations by the boundary element method", *Int. J. Num. Meth. Fluids*, Vol. 39, pp. 115-39.

Skerget, L. and Samec, N. (1999), "BEM for non-Newtonian flow", *Engineering Analysis with Boundary Elements*, Vol. 23 Nos 5-6, pp. 435-43.

Taigbenu, A.E. (1995), "The Green element method", *Int. J. Numer. Methods Eng.*, pp. 2241-63.

## Appendix. Particular solutions used in DRM

| Interpolation function $f^m(x)$ | Particular solution $\hat{T}_m$ |
|---|---|
| $r^2 \log r$ | $\frac{r^4 \log r}{16} - \frac{r^4}{32}$ |
| 1 | $\frac{x_1^2 + x_2^2}{4}$ |
| $x_1$ | $\frac{x_1^3 + x_1 x_2^2}{8}$ |
| $x_2$ | $\frac{x_2^3 + x_2 x_1^2}{8}$ |

**Table AI.** Particular solutions $\hat{T}_m$ for the DRM method and the energy equation

| Interpolation function $f^m(x)$ | Particular solution $\hat{q}_m$ |
|---|---|
| $r^2 \log r$ | $\frac{r^2 \hat{x}_i n_i \log r}{4} - \frac{r^2 \hat{x}_i n_i}{16}$<br>$\hat{x}_i = x_i - y_i^m$ |
| 1 | $\frac{x_1 \delta_{1i} + x_2 \delta_{2i}}{2} n_i$ |
| $x_1$ | $\frac{(3x_1^2 + x_2^2)\delta_{1i} + 2x_2 x_1 \delta_{2i}}{8} n_i$ |
| $x_2$ | $\frac{(3x_2^2 + x_1^2)\delta_{2i} + 2x_1 x_2 \delta_{1i}}{8} n_i$ |

**Table AII.** Particular solutions $\hat{q}_m$ for the DRM method and the energy equation

| Interpolation function $f^m(x)$ | Particular solution $\hat{u}_i^j$ |
|---|---|
| $r^2 \log r$ | $\hat{U}_i^j = \frac{1}{96\mu}\left[\left(5r^4 \log r - \frac{7}{3} r^4\right)\delta_{ij} - \hat{x}_i \hat{x}_j \left(4r^2 \log r - \frac{5}{3} r^2\right)\right]$<br>$\hat{x} = x - y^m \quad r = \lvert\hat{x}\rvert$ |
| 1 | $\hat{U}_i^j = \frac{1}{16}(3\lvert x\rvert^2 \delta_{ij} - 2x_i x_j)$ |
| $x_1$ | $\hat{U}_i^j = \frac{1}{24}\left[x_1^3(3\delta_{ij} - 2\delta_{1i}\delta_{1j} - \delta_{2i}\delta_{2j}) + 3x_2^2 x_1(\delta_{ij} - \delta_{1i}\delta_{1j}) - 3x_1^2 x_2(\delta_{1i}\delta_{2j} + \delta_{2i}\delta_{1j})\right]$ |
| $x_2$ | $\hat{U}_i^j = \frac{1}{24}\left[x_2^3(3\delta_{ij} - 2\delta_{2i}\delta_{2j} - \delta_{1i}\delta_{1j}) + 3x_1^2 x_2(\delta_{ij} - \delta_{2i}\delta_{2j}) - 3x_2^2 x_1(\delta_{2i}\delta_{1j} + \delta_{1i}\delta_{2j})\right]$ |

**Table AIII.** Particular solutions $\hat{u}_i^j$

| Interpolation function $f^m(x)$ | Particular solution $\hat{t}_i^k$ |
|---|---|
| $r^2 \log r$ | $\hat{t}_i^k = \frac{1}{96}\left[8r^2(\hat{x}_i n_k + \hat{x}_j n_j \delta_{ik} + \hat{x}_k n_i)\left(2\log r - \frac{1}{3}\right)\right.$ $\left. -4\hat{x}_i \hat{x}_k \hat{x}_j n_j \left(4\log r + \frac{1}{3}\right)\right]$ |
| 1 | $\hat{t}_i^k = \frac{1}{4}[x_i n_k + x_j n_j \delta_{ik} + x_k n_i]$ |
| $x_1$ | $\hat{t}_i^k = \frac{1}{8}\{x_1^2[3(n_1\delta_{ik} + n_k\delta_{1i} + n_i\delta_{1k})$ $-2(2n_1\delta_{1i}\delta_{1k} + n_1\delta_{2i}\delta_{2k} + n_2\delta_{1i}\delta_{2k} + n_2\delta_{1k}\delta_{2i})]$ $+x_2^2[n_1\delta_{ik} + n_k\delta_{1i} + n_i\delta_{1k} - 2n_1\delta_{1i}\delta_{1k}]$ $+2x_1x_2[(n_2\delta_{ik} + n_k\delta_{2i} + n_i\delta_{2k})$ $-2(n_2\delta_{1i}\delta_{1k} + n_1\delta_{1i}\delta_{2k} + n_1\delta_{1k}\delta_{2i})]\}$ |
| $x_2$ | $\hat{t}_i^k = \frac{1}{8}\{x_2^2[3(n_2\delta_{ik} + n_k\delta_{2i} + n_i\delta_{2k})$ $-2(2n_2\delta_{2i}\delta_{2k} + n_2\delta_{1i}\delta_{1k} + n_1\delta_{2i}\delta_{1k} + n_1\delta_{2k}\delta_{1i})]$ $+x_1^2[n_2\delta_{ik} + n_k\delta_{2i} + n_i\delta_{2k} - 2n_2\delta_{2i}\delta_{2k}]$ $+2x_1x_2[(n_1\delta_{ik} + n_k\delta_{1i} + n_i\delta_{1k})$ $-2(n_2\delta_{2i}\delta_{1k} + n_1\delta_{2i}\delta_{2k} + n_2\delta_{2k}\delta_{1i})]\}$ |

**Table AIV.**
Particular solution for the traction $\hat{t}_i^k$